Quantum theory of multiwave mixing. III. Averages over inhomogeneous broadening, spatial hole burning, and Gaussian beams

David A. Holm, Murray Sargent III, and Lois M. Hoffer
Optical Sciences Center, University of Arizona, Tucson, Arizona 85721
(Received 2 April 1985)

The effects of inhomogeneous broadening, spatial hole burning, and Gaussian beams are calculated for the four coefficients derived in previous papers in this series [Phys. Rev. A 31, 3112 (1985); 31, 3124 (1985)] on the quantum theory of multiwave mixing. These coefficients uniformly describe how one or two strong classical-field modes and one or two weak quantum-field modes interact in a two-level medium. The phenomena for which this theory is applicable includes resonance fluorescence, Rayleigh scattering, laser and/or optical bistability instabilities, and phase conjugation. The averaged formulas are illustrated by resonance-fluorescence spectra. We find the sidepeaks can be "washed out" and that asymmetries can occur.

I. INTRODUCTION

In two recent papers[1,2] a quantum theory of multiwave interactions with a two-level medium is presented. The theory is able to treat a number of topics in quantum optics involving nonlinear interactions with several fields, including resonance-fluorescence, saturation spectroscopy, laser and optical bistability instabilities, and three- and four-wave mixing. It can be applied to cavity problems, showing how stimulated emission alters the spontaneous emission spectrum, and to propagation problems, revealing how quantum noise influences the emergent beam.

The theory assumes that a homogeneously broadened medium interacts with one classical-plane running wave of arbitrary intensity and one or two weak-quantized-plane running waves. In this paper we separately study the effects of (i) inhomogeneous broadening, (ii) spatial hole burning resulting from a standing-wave pump field, and (iii) Gaussian transverse-amplitude variations. By treating them separately we obtain analytic formulas for the averaged coefficients. Numerical analysis is required to perform a second average. In particular, since resonance fluorescence is a special case of the theory, we primarily consider how the well-known three-peaked spectrum of resonance fluorescence is altered by these effects.

Inhomogeneous broadening occurs in many media of interest in phase conjugation, lasers, optical bistability, and saturation spectroscopy. In particular, the laser instabilities have usually required inhomogeneous broadening for observation.[3–5] Saturation spectroscopy is often done with gaseous media having Doppler broadening. Experiments are done in atomic beams and for two-photon transitions to observe phenomena masked in classical spectroscopy by the Doppler effect.[6] Our calculations allow some of these effects to be studied more easily with the naturally inhomogeneously broadened state. Standing waves are important both in cavity problems and in using four-wave mixing to achieve phase conjugation.[7,8] Gaussian beams are almost always encountered in nonlinear wave mixing,[9,10] although the effects of transverse variations can be discriminated against by appropriate use of apertures. Our formulas can help in estimating the kinds of effects that such transverse variations have on a number of common multiwave interactions. We illustrate all three averages numerically with their effects on resonance fluorescence.[11,12] Further illustrations will be given in the fourth paper in this series, which will discuss the effects of cavities on the spectrum of resonance fluorescence.[13]

The theoretical derivation of Ref. 1 uses a two-excited-level model with a lower-lying ground state as depicted in Fig. 1. The field modes of interest cause transitions between levels a and b, while level c acts as a reservoir connected by level decays and pumps. γ_a and γ_b are the rates at which levels a and b decay to level c, and Λ_a and Λ_b are the pumping rates from level c to a and b. Γ describes the decay from level a to b. The use of this level scheme makes the equations substantially more algebraically complex than the usual two-level upper- to ground-level model generally assumed for these problems. However, this level scheme allows us to treat transitions between two excited states as well the upper- to ground-level model, all with a unified notation. As we show, this flexibility has some interesting consequences when inhomogeneous broadening is considered. To obtain the upper- to ground-level model from our three-level model, simply set $\gamma_a=\gamma_b=0$. Another special case of interest occurs when levels a and b are both excited, but most of the atoms are in the reservoir c. This limit is usually considered for lasers,[14] and for this $\Gamma=0$ and $\Lambda_a,\Lambda_b \ll \gamma_a,\gamma_b$. Although our averaged coefficients are valid for all values of the pumping and decay constants, we confine our numerical illustrations to these special cases.

Section II summarizes the theoretical calculations presented in Ref. 1. Section III carries out the average over inhomogeneous broadening using a Lorentzian distribution function. This allows us to study the transition from homogeneous broadening to strong inhomogeneous broadening with an analytic function. Section IV averages the coefficients over a standing wave, appropriate for use in four-wave mixing and in standing-wave cavity

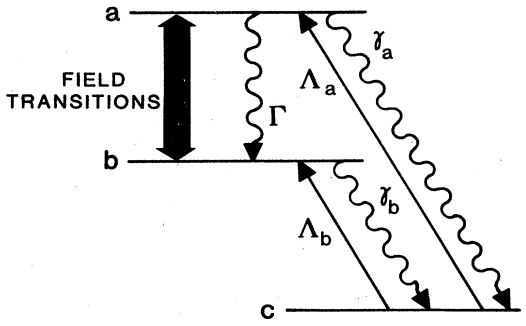

FIG. 1. Three-level atomic energy-level scheme that treats both purely excited-state interactions as well as upper- to ground-level interactions in a uniform way.

problems. Section V averages the coefficients over a Gaussian beam that approximates the transverse-field distribution often produced by lasers.

II. SUMMARY OF BASIC EQUATIONS

Our Hamiltonian (in radians/second) is

$$H=(\omega-\nu_2)\sigma_z+\sum_{j=1}^{3}[(\nu_j-\nu_2)a_j^\dagger a_j+(ga_jU_j\sigma^\dagger+\text{H.c.})]\ . \tag{1}$$

In this expression a_j is the annihilation operator for the jth field mode, $U_j=U_j(\mathbf{r})$ is the corresponding spatial mode factor, σ and σ_z are the atomic spin-flip and probability-difference operators, ω and ν_j are the atomic and field frequencies, and g is the atom-field coupling constant. As in the semiclassical theories,[15] mode 2 can be arbitrarily intense, and is treated classically. Modes 1 and 3 are quantum fields treated only to second order in amplitude. As such they cannot by themselves saturate the atomic response. The rotating-wave approximation has been made and this Hamiltonian is in an interaction picture rotating at the strong-field frequency ν_2. We define an atom-field density operator ρ_{a-f} and obtain its time dependence from the standard density-operator equation of motion

$$\dot{\rho}_{a-f}=-i[H,\rho_{a-f}]+\cdots\ , \tag{2}$$

where the ellipsis represents unspecified decay and pumping terms. We calculate the reduced two-mode-field density operator ρ to describe the time dependence of the two quantized fields by taking the trace of ρ_{a-f} over the atomic states. As in semiclassical laser theory,[14] we consider all field amplitudes to vary little in atomic decay times. This allows us to solve the atomic equations of motion in steady state, and then to obtain a slowly varying-field sidemode density-operator equation of motion

$$\dot{\rho}=\{[-A_1(\rho a_1a_1^\dagger-a_1^\dagger\rho a_1)-(B_1+\nu/2Q_1)(a_1^\dagger a_1\rho-a_1\rho a_1^\dagger)+C_1(a_1^\dagger a_3^\dagger\rho-a_3^\dagger\rho a_1^\dagger)+D_1(\rho a_3^\dagger a_1^\dagger-a_1^\dagger\rho a_3^\dagger)]+[1\leftrightarrow3]+\text{H.c.}\} \tag{3}$$

where ν/Q_n is the cavity-loss rate for mode n and the coefficients A_1, B_1, C_1, and D_1 are given by

$$A_1=\frac{g^2\mathscr{D}_1}{1+I_2\mathscr{L}_2}\left[f_a-\frac{I_2\frac{\gamma}{2}[f_a\mathscr{F}\mathscr{D}_1+(N_a-N_b)\mathscr{D}_2^*(\mathscr{D}_0-\mathscr{S}/i\Delta)/2T_1]}{1+I_2\mathscr{F}\frac{\gamma}{2}(\mathscr{D}_1+\mathscr{D}_3^*)}\right], \tag{4}$$

$$B_1=\frac{g^2\mathscr{D}_1}{1+I_2\mathscr{L}_2}\left[f_b-\frac{I_2\frac{\gamma}{2}[f_b\mathscr{F}\mathscr{D}_1-(N_a-N_b)\mathscr{D}_2^*(\mathscr{D}_a+\mathscr{S}/i\Delta)/2T_1]}{1+I_2\mathscr{F}\frac{\gamma}{2}(\mathscr{D}_1+\mathscr{D}_3^*)}\right], \tag{5}$$

$$C_1=-\frac{g^2\mathscr{D}_1}{1+I_2\mathscr{L}_2}U_1^*U_3^*V_2^2\frac{2T_1\mathscr{F}\mathscr{D}_3^*f_a+(N_a-N_b)\mathscr{D}_2(\mathscr{D}_b-\mathscr{S}/i\Delta)}{1+I_2\mathscr{F}\frac{\gamma}{2}(\mathscr{D}_1+\mathscr{D}_3^*)}, \tag{6}$$

$$D_1=-\frac{g^2\mathscr{D}_1}{1+I_2\mathscr{L}_2}U_1^*U_3^*V_2^2\frac{2T_1\mathscr{D}_3^*\mathscr{F}f_b-(N_a-N_b)\mathscr{D}_2(\mathscr{D}_b+\mathscr{S}/i\Delta)}{1+I_2\mathscr{F}\frac{\gamma}{2}(\mathscr{D}_1+\mathscr{D}_3^*)}, \tag{7}$$

where, following the notation of Ref. 1, the complex Lorentzian denominators $\mathscr{D}_n$ are given by

$$\mathscr{D}_n=\frac{1}{\gamma+i(\omega-\nu_n)}\ ,$$

the dimensionless Lorentzian $\mathscr{L}_2$ is

$$\mathscr{L}_2=\frac{\gamma^2}{\gamma^2+(\omega-\nu_2)^2}\ ,$$

and the unsaturated probabilities of being in the upper and lower levels are

$$N_a=\frac{\Lambda_a\gamma_b}{\gamma_a\gamma_b+\gamma_a\Lambda_b+\gamma_b\Lambda_a+\Gamma(\gamma_b+\Lambda_a+\Lambda_b)},\quad N_b=\frac{\Lambda_b\gamma_a+(\Lambda_a+\Lambda_b)\Gamma}{\gamma_a\gamma_b+\gamma_a\Lambda_b+\gamma_b\Lambda_a+\Gamma(\gamma_b+\Lambda_a+\Lambda_b)}.$$

The effective upper- and lower-level decay constants γ'_a and γ'_b are

$$\gamma'_a=\gamma_a+\Gamma+\frac{\Lambda_a(\gamma_b-\gamma_a)}{\gamma_b+\Lambda_a+\Lambda_b},\quad \gamma'_b=\gamma_b+\frac{\Gamma(\gamma_b+\Lambda_a+\Lambda_b)+\Lambda_b(\gamma_a-\gamma_b)}{\gamma_a+\Lambda_a+\Lambda_b}.$$

The other quantities are then given by

$$T_1=\tfrac{1}{2}\left[\frac{1}{\gamma_{a'}}+\frac{1}{\gamma_{b'}}\right],\quad T_2=\frac{1}{\gamma},\quad I_2=4|V_2|^2T_1T_2,$$

$$f_a=\left[1+\frac{I_2\mathscr{L}_2}{2T_1\gamma'_b}\right]N_a+\frac{I_2\mathscr{L}_2}{2T_1\gamma'_a}N_b,\quad f_b=\frac{I_2\mathscr{L}_2}{2T_1\gamma'_b}N_a+\left[1+\frac{I_2\mathscr{L}_2}{2T_1\gamma'_a}\right]N_b,$$

$$\mathscr{D}_a=\frac{\gamma_b+\Lambda_a+\Lambda_b+i\Delta}{(\gamma_a+i\Delta)(\gamma_b+i\Delta)+(\gamma_a+i\Delta)\Lambda_b+(\gamma_b+i\Delta)\Lambda_a+(\gamma_b+\Lambda_a+\Lambda_b+i\Delta)\Gamma},$$

$$\mathscr{D}_b=\frac{\gamma_a+\Lambda_a+\Lambda_b+i\Delta}{(\gamma_a+i\Delta)(\gamma_b+i\Delta)+(\gamma_a+i\Delta)\Lambda_b+(\gamma_b+i\Delta)\Lambda_a+(\gamma_b+\Lambda_a+\Lambda_b+i\Delta)\Gamma},$$

$$\mathscr{F}=\frac{1}{2T_1}(\mathscr{D}_a+\mathscr{D}_b),$$

$$\mathscr{S}=\frac{\Lambda_a\gamma_b-\Lambda_b\gamma_a-(\Lambda_a+\Lambda_b+i\Delta)\Gamma}{(\gamma_a+i\Delta)(\gamma_b+i\Delta)+(\gamma_a+i\Delta)\Lambda_b+(\gamma_b+i\Delta)\Lambda_a+(\gamma_b+\Lambda_a+\Lambda_b+i\Delta)\Gamma},$$

where $V_2=gU_2\sqrt{n_2+1}$, and $\Delta=\nu_2-\nu_1$ is the beat frequency between modes 1 and 2.

As shown in Refs. 1 and 2, A_1 + c.c. yields the spectrum of resonance fluorescence, while A_1-B_1 is the semiclassical complex gain and/or absorption coefficient α_1 for a weak probe field in the presence of a saturating field, and C_1-D_1 is the semiclassical complex-coupling coefficient $i\kappa_1$ between the signal and conjugate fields in phase conjugation. We calculate the three averages for A_1, B_1, C_1, and D_1, and illustrate the resonance-fluorescence spectrum A_1 + c.c. numerically.

III. INHOMOGENEOUS BROADENING

In this section we include inhomogeneous broadening for our theoretical model. We integrate each coefficient over the inhomogeneous broadening function $W(\omega)$. Specifically, the inhomogeneously broadened resonance-fluorescence coefficient A_1 is given by

$$\langle A_1\rangle_{\rm IHB}=\int_{-\infty}^{\infty}d\omega\,W(\omega)A_1(\omega),\tag{8}$$

where $W(\omega)$ is the inhomogeneous-broadening function. For very large inhomogeneous broadening, i.e., a distribution with width many times that of the homogeneous width γ, $W(\omega)$ may be evaluated at the peak of $A_1(\omega)$ and pulled out of the integral in Eq. (8). This procedure is similar to that discussed in the semiclassical theory of Ref. 15. In order to study the transition from homogeneous to inhomogeneous broadening analytically, we assume $W(\omega)$ is given by the Lorentzian

$$W(\omega)=\frac{w}{\pi}\frac{1}{w^2+(\omega-\nu_2)^2},\tag{9}$$

with full width at half maximum (FWHM) of $2w$ as in the work of Mandel.[5] In the limit $w\to 0$, $W(\omega)\to\delta(\omega-\nu_2)$, which reduces Eq. (8) to the centrally tuned homogeneous broadening result. The limit $w\to\infty$ gives large inhomogeneous broadening. To keep $\langle A_1\rangle_{\rm IHB}$ from vanishing in the inhomogeneously broadened limit while reducing properly to the homogeneously broadened case, we multiply by the normalization factor $Z=(w+\gamma)/\gamma$.

Following the notation of Ref. 15, we define $\delta=\omega-\nu_2$, $\gamma'=\gamma\sqrt{1+I_2}$, and $\beta^2=(\gamma+i\Delta)(\gamma+i\Delta+\gamma I_2\mathscr{F})$. Isolating the terms that depend upon the detuning δ, we find that the integrals for A_1 and B_1 can be broken into five separate terms while those for C_1 and D_1 can be broken in three separate terms. Each term in the integral can then be evaluated by the calculus of residues.

The results of these calculations yield

$$\langle A_1\rangle_{\rm IHB}=g^2Z[N_a\mathscr{W}_{\rm I}+M_{ab}\mathscr{W}_{\rm II}+N_a(\mathscr{W}_{\rm III})_1+M_{ab}(\mathscr{W}_{\rm IV})_1+K_b(\mathscr{W}_{\rm V})_{AB}],\tag{10}$$

$$\langle B_1\rangle_{\rm IHB}=g^2Z[N_b\mathscr{W}_{\rm I}+M_{ab}\mathscr{W}_{\rm II}+N_b(\mathscr{W}_{\rm III})_1+M_{ab}(\mathscr{W}_{\rm IV})_1+K_a(\mathscr{W}_{\rm V})_{AB}],\tag{11}$$

$$\langle C_1\rangle_{\rm IHB}=g^2ZU_1^*U_3^*[N_a(\mathscr{W}_{\rm III})_3+M_{ab}(\mathscr{W}_{\rm IV})_3+K_b(\mathscr{W}_{\rm V})_{CD}]\ , \tag{12}$$

$$\langle D_1\rangle_{\rm IHB}=g^2ZU_1^*U_3^*[N_b(\mathscr{W}_{\rm III})_3+M_{ab}(\mathscr{W}_{\rm IV})_3+K_a(\mathscr{W}_{\rm V})_{CD}]\ , \tag{13}$$

where

$$\mathscr{W}_{\rm I}=-\frac{w}{w^2-\gamma'^2}\left[\frac{\gamma'^2-\gamma^2}{\gamma'(\gamma'+\gamma+i\Delta)}-\frac{w^2-\gamma^2}{w(w+\gamma+i\Delta)}\right], \tag{14}$$

$$\mathscr{W}_{\rm II}=\frac{\gamma^2 w}{w^2-\gamma'^2}\left[\frac{1}{\gamma'(\gamma'+\gamma+i\Delta)}-\frac{1}{w(w+\gamma+i\Delta)}\right], \tag{15}$$

$$(\mathscr{W}_{\rm III})_1=\frac{\gamma I_2\mathscr{F}w}{2}\left[\frac{1}{\gamma'^2-\beta^2}\left[\frac{(\gamma'^2-\gamma^2)(\gamma'-\gamma-i\Delta)}{\gamma'(\gamma'+\gamma+i\Delta)(w^2-\gamma'^2)}-\frac{(\beta^2-\gamma^2)(\beta-\gamma-i\Delta)}{\beta(\beta+\gamma+i\Delta)(w^2-\beta^2)}\right]-\frac{(w^2-\gamma^2)(w-\gamma-i\Delta)}{w(w+\gamma+i\Delta)(w^2-\gamma'^2)(w^2-\beta^2)}\right], \tag{16}$$

$$(\mathscr{W}_{\rm III})_3=-2T_1V_2^2\mathscr{F}w\left[\frac{1}{\gamma'^2-\beta^2}\left[\frac{\gamma'^2-\gamma^2}{\gamma'(w^2-\gamma'^2)}-\frac{\beta^2-\gamma^2}{\beta(w^2-\beta^2)}\right]-\frac{w^2-\gamma^2}{w(w^2-\gamma'^2)(w^2-\beta^2)}\right], \tag{17}$$

$$(\mathscr{W}_{\rm IV})_1=-\frac{\gamma^3I_2\mathscr{F}w}{2}\left[\frac{1}{\gamma'^2-\beta^2}\left[\frac{\gamma'-\gamma-i\Delta}{\gamma'(\gamma'+\gamma+i\Delta)(w^2-\gamma'^2)}-\frac{\beta-\gamma-i\Delta}{\beta(\beta+\gamma+i\Delta)(w^2-\beta^2)}\right]-\frac{w-\gamma-i\Delta}{w(w+\gamma+i\Delta)(w^2-\gamma'^2)(w^2-\beta^2)}\right], \tag{18}$$

$$(\mathscr{W}_{\rm IV})_3=2T_1V_2^2\gamma^2\mathscr{F}w\left[\frac{1}{\gamma'^2-\beta^2}\left[\frac{1}{\gamma'(w^2-\gamma'^2)}-\frac{1}{\beta(w^2-\beta^2)}\right]-\frac{1}{w(w^2-\gamma'^2)(w^2-\beta^2)}\right], \tag{19}$$

$$(\mathscr{W}_{\rm V})_{AB}=-\frac{\gamma I_2 w}{2}\left[\frac{1}{\gamma'^2-\beta^2}\left[\frac{(\gamma'+\gamma)(\gamma'-\gamma-i\Delta)}{\gamma'(w^2-\gamma'^2)}-\frac{(\beta+\gamma)(\beta-\gamma-i\Delta)}{\beta(w^2-\beta^2)}\right]-\frac{(w+\gamma)(w-\gamma-i\Delta)}{w(w^2-\gamma'^2)(w^2-\beta^2)}\right], \tag{20}$$

$$(\mathscr{W}_{\rm V})_{CD}=2T_1V_2^2w\left[\frac{1}{\gamma'^2-\beta^2}\left[\frac{(\gamma'-\gamma)(\gamma'-\gamma-i\Delta)}{\gamma'(w^2-\gamma'^2)}-\frac{(\beta-\gamma)(\beta-\gamma-i\Delta)}{\beta(w^2-\beta^2)}\right]-\frac{(w-\gamma)(w-\gamma-i\Delta)}{w(w^2-\gamma'^2)(w^2-\beta^2)}\right], \tag{21}$$

where

$$M_{ab}=\frac{I_2}{2T_1}\left[\frac{N_a}{\gamma_{b'}}+\frac{N_b}{\gamma_{a'}}\right],\quad K_a=-\frac{N_a-N_b}{2T_1}\left[\mathscr{D}_a+\frac{\mathscr{S}}{i\Delta}\right],\quad\text{and } K_b=\frac{N_a-N_b}{2T_1}\left[\mathscr{D}_b-\frac{\mathscr{S}}{i\Delta}\right].$$

We now compare these results to previous semiclassical calculations[15] by taking the differences $\langle A_1-B_1\rangle_{\rm IHB}$ and $\langle C_1-D_1\rangle_{\rm IHB}$. In Ref. 15, only large inhomogeneous broadening was considered, so we allow $w\to\infty$ in our expressions. For the absorption coefficient, we have

$$\langle A_1-B_1\rangle_{\rm IHB}=g^2(N_a-N_b)(\mathscr{W}_{\rm I})+(\mathscr{W}_{\rm III})_1+\mathscr{F}(\mathscr{W}_{\rm V})_{AB})\ . \tag{22}$$

Letting $w\to\infty$ in the terms in Eq. (22) this expression becomes

$$\langle A_1-B_1\rangle_{\rm IHB}=-g^2(N_a-N_b)\left[\frac{\gamma'^2-\gamma^2}{\gamma\gamma'(\gamma'+\gamma+i\Delta)}+\frac{I_2\mathscr{F}(2\gamma+i\Delta)}{2(\gamma'^2-\beta^2)}\left[\frac{(\gamma'+\gamma)(\gamma'-\gamma-i\Delta)}{\gamma'(\gamma'+\gamma+i\Delta)}-\frac{(\beta+\gamma)(\beta-\gamma-i\Delta)}{\beta(\beta+\gamma+i\Delta)}\right]\right]. \tag{23}$$

Similarly, we subtract $\langle D_1\rangle_{\rm IHB}$ from $\langle C_1\rangle_{\rm IHB}$ and let $w\to\infty$. Then

$$\langle C_1-D_1\rangle_{\rm IHB}=\frac{g^2U_1^*U_3^*(N_a-N_b)(2T_1V_2^2\mathscr{F})(2\gamma+i\Delta)}{\gamma'\beta(\gamma'+\beta)}\ . \tag{24}$$

Equations (23) and (24) agree with the semiclassical calculations of Ref. 15, Eqs. (74) and (76), as they should.

We now consider two limiting cases to analyze these results. First consider upper- to ground-level decay. Figure 2 shows the resonance-fluorescence spectrum as a function of ΔT_1 for the case of $T_2=2T_1=2/\Gamma$, and an intensity I_2 of 50 for $w=0$, $1/T_1$, and $10000/T_1$. The overall height of the curve rises a little due to our normalization factor $(w+\gamma)/\gamma$. Note, however, that even for the small amount of inhomogeneous broadening, $w=1/T_1$, the sidebands have moved further out and have a higher sideband-to-central-peak height ratio than the homogeneously broadened case. For inhomogeneous

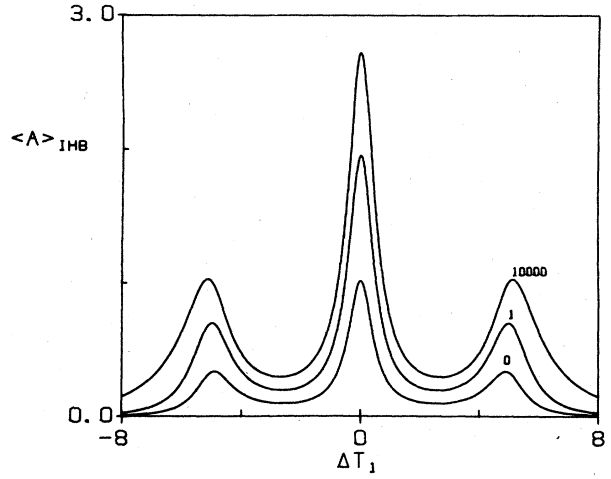

FIG. 2. Resonance-fluorescence spectra vs $(\nu_2-\nu_1)T_1=\Delta T_1$ for inhomogeneous distribution widths $w=0,1/T_1,10000/T_1$. The lower level is the ground state, the pump intensity I_2 is 50, and $T_2=2T_1$.

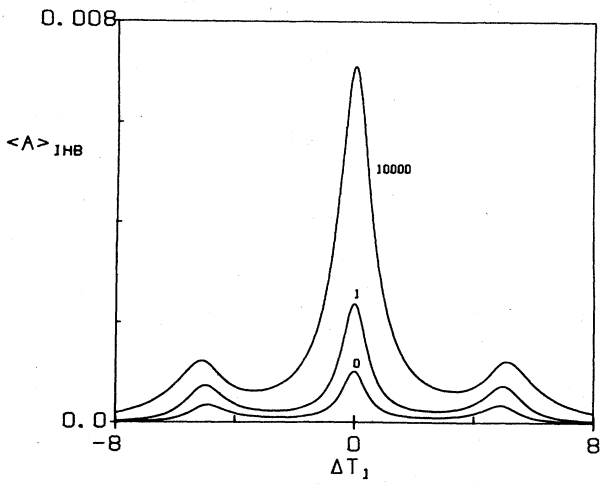

FIG. 4. Resonance-fluorescence spectra vs ΔT_1 for inhomogeneous distribution widths $w=0,1/T_1,10000/T_1$. Both levels are excited and there is pumping to only the lower level. The intensity I_2 is 50, and $T_2=2T_1$.

broadening we are combining a distribution of off-resonance quantities. For the case of resonance fluorescence, it is well known that the spectrum remains fully symmetric even off resonance for the case of upper- to ground-level decay.[11] The central peak of the inelastic spectrum rapidly falls off with detuning and the sidebands move further out to the detuned Rabi flopping frequency. This is shown in Fig. 3 for detunings of $\delta=0$, $2/T_1$, and $5/T_1$. Since the central peak falls off more rapidly than the sidebands, this explains why the sidebands increase in height relative to the central peak for large inhomogeneous broadening.

Figure 4 shows the resonance-fluorescence spectrum for a two-level system with both levels excited. For this case there is incoherent pumping to only the lower level and most of the atoms are in the reservoir level c. Specifically, $\gamma_a=\gamma_b=2\gamma$, $\Gamma=\Lambda_a=0$, $\Lambda_b=0.001\gamma_a$, and the spectrum is again plotted versus ΔT_1 for $I_2=50$ and $w=0$, $1/T_1$, and $10000/T_1$. Note how much higher the central peak is relative to the sidebands, which is remarkably different than for the upper- to ground-level decay of Fig. 2. Figure 5 depicts the off-resonant spectrum for this case with the same detunings of $\delta=0$, $2/T_1$, and $5/T_1$. Note that now the spectrum becomes slightly asymmetric with detuning, but more importantly the central peak does not fall off as rapidly as in Fig. 3. These results are in agreement with earlier calculations for this case.[16]

Finally, we again consider an excited two-level system as in Fig. 4, only now we let $\Lambda_a=0.001\gamma_a$ and $\Lambda_b=0$, with everything else unchanged. The curves depicted in Fig. 6 are considerably different from the previous cases. The upper-level excitation gives increasing larger wings due to the introduction of unsaturated atoms. The off-resonance curves of Fig. 7 are also very different. Because of spontaneous emission from level a resulting from the incoherent pump Λ_a, the spectrum is now asymmetric off

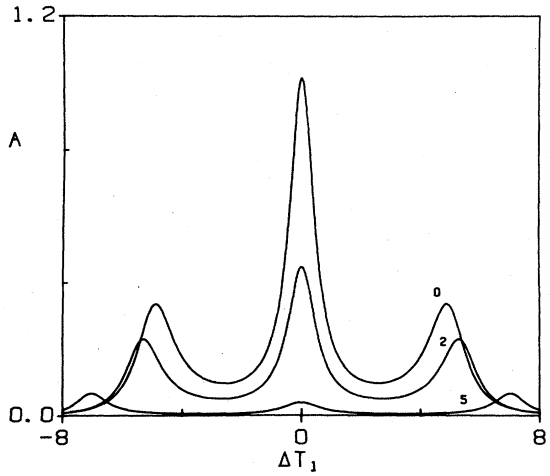

FIG. 3. Resonance-fluorescence spectra vs ΔT_1 for detunings $\delta=0$, $2/T_1$, and $5/T_1$. Other parameters are the same as for Fig. 2.

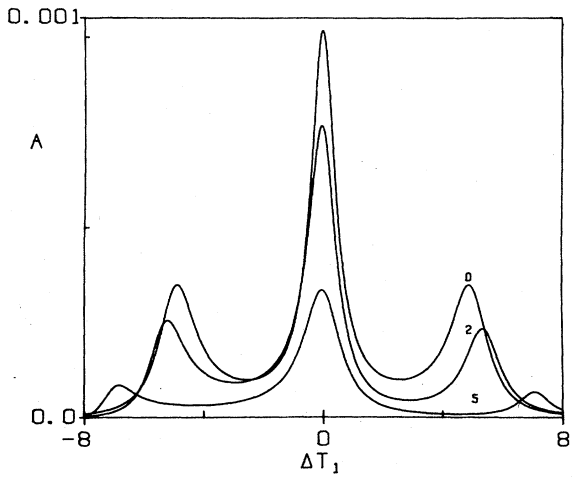

FIG. 5. Detuned spectra vs ΔT_1 for the parameters of Fig. 4 with detunings $\delta=0$, $2/T_1$, and $5/T_1$.

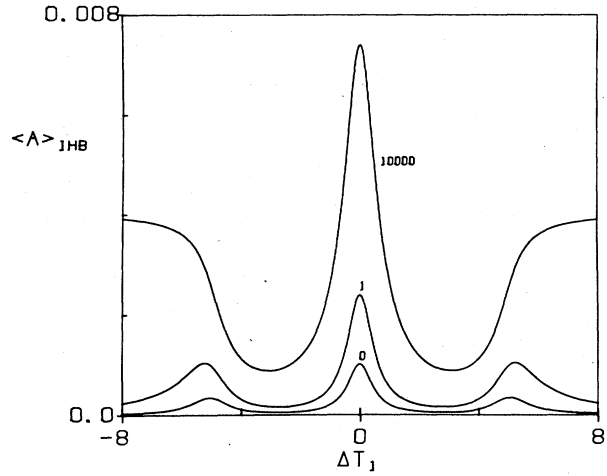

FIG. 6. Spectra vs ΔT_1 for $w=0$, $1/T_1$, and $10000/T_1$ when both levels are excited and there is pumping to only the upper level. Note the wide wings due to the introduction of unsaturated atoms as w increases.

resonance. Note, however, that all values of the detuning have a residual peak at the center, thereby giving the increased peak at line center in the inhomogeneously broadened case just as for the lower-level excitation case.

The $\mathscr{S}/i\Delta$ term in Eq. (4) is primarily responsible for two differences in scattering predicted by the upper- to ground-level decay model and by the large-reservoir excited-state model appropriate for typical laser media. First, because of the presence of the Lorentzian factor $I_2\mathscr{L}_2$ in f_a, the term proportional to $\mathscr{D}_2^*$ becomes dominant for sufficiently large detunings. For upper- to ground-level decay, $\mathscr{S}=-\Gamma/(\Gamma+i\Delta)$ and is on the order of unity, and hence gives an important contribution. However, for the large-reservoir excited-state model, $\mathscr{S}$ is given by

$$\mathscr{S}\simeq\frac{\Lambda_a\gamma_b-\Lambda_b\gamma_a}{(\gamma_a+i\Delta)(\gamma_b+i\Delta)}\ ,$$

and the pump-rate constants satisfy

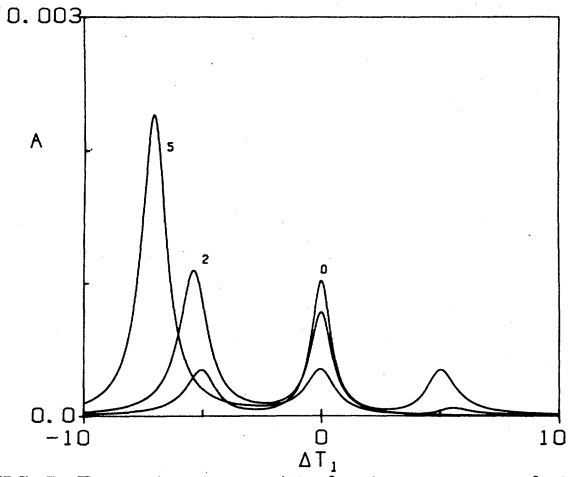

FIG. 7. Detuned spectra vs ΔT_1 for the parameters of Fig. 6 with detunings $\delta=0$, $2/T_1$, and $5/T_1$.

$$\Lambda_{a,b}\ll\gamma_{a,b}\ .$$

Hence this $\mathscr{S}$ gives a negligible contribution.

Second, the $\mathscr{S}/i\Delta$ term also leads to the elastic, or Rayleigh, peak not shown in these curves. This is because the resonance-fluorescence scattering is proportional to A_1 + c.c., which due to the $\mathscr{S}/i\Delta$ term contains a contribution proportional to i/Δ+c.c. $=2\pi\delta(\Delta)$. This monochromatic scattering constitutes the Rayleigh scattering. Hence in contrast to the upper- to ground-level model, the large-reservoir excited-state model has negligible Rayleigh scattering.

To study the effects of inhomogeneous broadening on Rayleigh scattering, we first evaluate the elastic peak for the homogeneous case by letting $\Delta=0$ in the $\mathscr{S}/i\Delta$ term and then use the above relationship. This gives

$$A_{\rm EL}=\frac{\pi g^2(N_a-N_b)^2}{2T_1\gamma}\frac{I_2\mathscr{L}_2}{(1+I_2\mathscr{L}_2)^2}\delta(\Delta)\ . \tag{25}$$

To include inhomogeneous broadening, we integrate this over ω times the Lorentzian distribution $W(\omega)$. Again using the calculus of residues, we find

$$\langle A_{\rm EL}\rangle_{\rm IHB}=\frac{\pi g^2 Z(N_a-N_b)^2\gamma I_2}{4T_1}\left[\frac{2\gamma'+w(2+I_2)}{\gamma'(w+\gamma')^2}\right]\delta(\Delta). \tag{26}$$

This reduces to the well-known centrally tuned homogeneously broadened value

$$\langle A_{\rm EL}\rangle_{\rm HB}=\frac{\pi g^2(N_a-N_b)^2 I_2}{2\gamma T_1(1+I_2)^2}\delta(\Delta)\ , \tag{27}$$

when $w=0$, which saturates to zero for large pump intensity I_2. In contrast the inhomogeneously broadened limit value

$$\langle A_{\rm EL}\rangle_{\rm IHB}=\frac{\pi g^2(N_a-N_b)^2\gamma I_2(2+I_2)}{4\gamma T_1\sqrt{1+I_2}}\delta(\Delta) \tag{28}$$

does not saturate, because of the contributions of the off-resonant dipoles. Equation (26) is plotted in Fig. 8 versus w for the upper- to ground-level case with $I_2=50$. From Fig. 8 we see that as w increases, the elastic contribution to the spectrum rapidly rises, dominating the total emission. As mentioned above, this term in the expression for A_1 is negligible for the large-reservoir excited-state limit appropriate for most lasers. Hence, Rayleigh scattering is not significant for this case. An interesting laser case that can exhibit substantial Rayleigh scattering is the ruby laser, whose lower level is the ground state.

IV. SPATIAL HOLE BURNING

In the semiclassical theory of resonant phase conjugation, one considers either three- or four-wave mixing. In three-wave mixing, a strong pump field interacts with a weak-signal probe field to generate another field. From phase matching considerations, all three fields must be nearly colinear. In four-wave mixing, two strong, oppositely directed pump fields interact with each other and the signal field to generate the fourth field. In this case

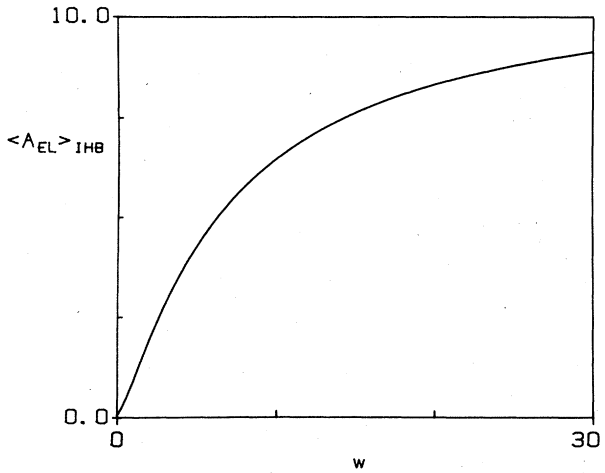

FIG. 8. The intensity of the elastic (Rayleigh) part of the spectrum vs the inhomogeneous width w and pump intensity $I_2=50$.

one of the pump fields and the signal field create a grating which scatters the other pump field into the opposite direction of the signal field. This provides the source for the conjugate wave and is phase matched for all wave vectors in the degenerate case $\nu_1=\nu_2=\nu_3$. Because of the two strong, saturating pump fields, however, a standing-wave fringe pattern exists in the medium. This subjects atoms at different locations in the fringe to different degrees of saturation. This is called spatial hole burning because the population difference follows the nodes and antinodes of the standing-wave electric field. We account for this by averaging the coefficients over the spatial hole burning for one wavelength. These results are of interest because it allows us to study resonant four-wave mixing from a quantum-mechanical viewpoint. The results are also useful in the theory of standing-wave cavity instabilities.

In this section we take the strong field E_2 to be a standing wave instead of a running wave. A standing-wave electric field is given by

$$E_2=\{\tfrac{1}{2}A_2\exp[i(\mathbf{K}_2\cdot\mathbf{r}-\nu_2 t)] + \tfrac{1}{2}A_2\exp[-i(\mathbf{K}_2\cdot\mathbf{r}+\nu_2 t)]\}+\text{c.c.} \tag{29}$$

We define the spatially dependent intensity as $\mathscr{I}_{2r}$ where

$$\mathscr{I}_{2r}=4\,|\,V_2\,|^2T_1T_2=\frac{4\mu^2\,|\,A_2\,|^2}{\hbar^2}\cos^2(\mathbf{K}_2\cdot\mathbf{r})T_1T_2 =4I_2\cos^2(\mathbf{K}_2\cdot\mathbf{r})\,, \tag{30}$$

where μ is the dipole moment, and I_2 is the dimensionless, running-wave pump intensity. For simplicity we take the wave vector $\mathbf{K}_2$ to be along the z axis, so $\mathbf{K}_2\cdot\mathbf{r}=K_2z=2\pi z/\lambda_2$. We integrate each coefficient along the z direction for one wavelength. For example,

$$\langle A_1\rangle_{\text{SHB}}=\frac{1}{\lambda_2}\int_0^{\lambda_2}dz\,A_1\,. \tag{31}$$

In the expressions for the four coefficients, Eqs. (4)—(7), we identify in each factor terms that depend upon the intensity I_2. We substitute Eq. (30) for I_2 and make use of the trigonometric identity $\cos^2(2K_2z)=[1+\cos(4K_2z)]/2$. With some algebra, the resulting integrals can all be reduced to combinations of the integral

$$J=\int_0^{2\pi}\frac{d\theta}{a+b\cos\theta}=\frac{1}{\sqrt{a^2-b^2}}\,.$$

We find

$$\langle A_1\rangle_{\text{SHB}}=\frac{g^2\mathscr{D}_1}{\mathscr{L}_2-d}\left[\frac{N_a\mathscr{L}_2-b_1+c/\mathscr{L}_2}{\sqrt{1+4I_2\mathscr{L}_2}}-\frac{N_ad-b_1+c/d}{\sqrt{1+4I_2d}}+c\left[\frac{1}{d}-\frac{1}{\mathscr{L}_2}\right]\right], \tag{32}$$

$$\langle B_1\rangle_{\text{SHB}}=\frac{g^2\mathscr{D}_1}{\mathscr{L}_2-d}\left[\frac{N_b\mathscr{L}_2-b_2+c/\mathscr{L}_2}{\sqrt{1+4I_2\mathscr{L}_2}}-\frac{N_bd-b_2+c/d}{\sqrt{1+4I_2d}}+c\left[\frac{1}{d}-\frac{1}{\mathscr{L}_2}\right]\right], \tag{33}$$

$$\langle C_1\rangle_{\text{SHB}}=-\frac{g^2U_1^*U_3^*\mathscr{D}_1}{\mathscr{L}_2-d}\left[\frac{-b_3+c/\mathscr{L}_2}{\sqrt{1+4I_2\mathscr{L}_2}}-\frac{-b_3+c/d}{\sqrt{1+4I_2d}}+c\left[\frac{1}{d}-\frac{1}{\mathscr{L}_2}\right]\right], \tag{34}$$

$$\langle D_1\rangle_{\text{SHB}}=-\frac{g^2U_1^*U_3^*\mathscr{D}_1}{\mathscr{L}_2-d}\left[\frac{-b_4+c/\mathscr{L}_2}{\sqrt{1+4I_2\mathscr{L}_2}}-\frac{-b_4+c/d}{\sqrt{1+4I_2d}}+c\left[\frac{1}{d}-\frac{1}{\mathscr{L}_2}\right]\right], \tag{35}$$

where

$$b_1=\frac{\mathscr{L}_2}{2T_1}\left[\frac{N_a}{\gamma_{b'}}+\frac{N_b}{\gamma_{a'}}\right]+\frac{\gamma}{2}\left[N_a\mathscr{F}\mathscr{D}_3^*-\frac{(N_a-N_b)\mathscr{D}_2^*}{2T_1}(\mathscr{D}_b-\mathscr{S}/i\Delta)\right], \tag{36}$$

$$b_2=\frac{\mathscr{L}_2}{2T_1}\left[\frac{N_a}{\gamma_{b'}}+\frac{N_b}{\gamma_{a'}}\right]+\frac{\gamma}{2}\left[N_b\mathscr{F}\mathscr{D}_3^*+\frac{(N_a-N_b)\mathscr{D}_2^*}{2T_1}(\mathscr{D}_a+\mathscr{S}/i\Delta)\right], \tag{37}$$

$$b_3=\frac{\gamma}{2}\left[N_a\mathscr{F}\mathscr{D}_3^*+\frac{(N_a-N_b)\mathscr{D}_2}{2T_1}(\mathscr{D}_b-\mathscr{S}/i\Delta)\right], \tag{38}$$

$$b_4=\frac{\gamma}{2}\left[N_b\mathcal{F}\mathcal{D}_3^*-\frac{(N_a-N_b)\mathcal{D}_2}{2T_1}(\mathcal{D}_a+\mathcal{S}/i\Delta)\right], \tag{39}$$

$$c=\frac{\gamma\mathcal{L}_2\mathcal{F}\mathcal{D}_3^*}{4T_1}\left[\frac{N_a}{\gamma_{b'}}+\frac{N_b}{\gamma_{a'}}\right], \tag{40}$$

$$d=\frac{\gamma}{2}\mathcal{F}(\mathcal{D}_1+\mathcal{D}_3^*). \tag{41}$$

Just as for inhomogeneous broadening, we calculate A_1-B_1 and C_1-D_1 and compare to previous semiclassical calculations.[8] Considerable simplification occurs for each case and we find

$$\langle A_1-B_1\rangle_{\rm SHB}=\frac{g^2\mathcal{D}_1(N_a-N_b)}{\sqrt{1+4I_2\mathcal{L}_2}}\left[1-\frac{2I_2\mathcal{F}\gamma(\mathcal{D}_1+\mathcal{D}_2^*)}{1+4I_2d+[(1+4I_2\mathcal{L}_2)(1+4I_2d)]^{1/2}}\right], \tag{42}$$

$$\langle C_1-D_1\rangle_{\rm SHB}=-\frac{g^2U_1^*U_3^*\mathcal{D}_1(N_a-N_b)2A_2\mathcal{F}\gamma(\mathcal{D}_2+\mathcal{D}_3^*)}{\sqrt{1+4I_2\mathcal{L}_2}\left[1+4I_2d+[(1+4I_2\mathcal{L}_2)(1+4I_2d)]^{1/2}\right]}. \tag{43}$$

These agree with the results of Ref. 8.

Equation (32) is the formula for resonance-fluorescence coefficient A_1 for a standing-wave pump field. Figure 9 plots the resonance-fluorescence spectrum $\langle A_1\rangle_{\rm SHB}+$c.c. of Eq. (32) for the upper- to ground-level case for $T_2=2T_1$ and intensities I_2 of 8, 18, and 50 for each pump field. Note that the central peaks for all three intensities are approximately the same and are much sharper and higher than the sidebands. Because the fluorescence is emitted by atoms in different locations in the standing-wave fringe, a distribution of Rabi sidebands contribute, tending to wash out the sidemode Lorentzians characteristic of the unidirectional case. However, all parts of the fringe contribute to the central frequency, reinforcing the central peak.

The elastic peak may also be evaluated in the same manner as for inhomogeneous broadening. Substituting Eq. (25) into Eq. (31) and integrating over one wavelength, we obtain

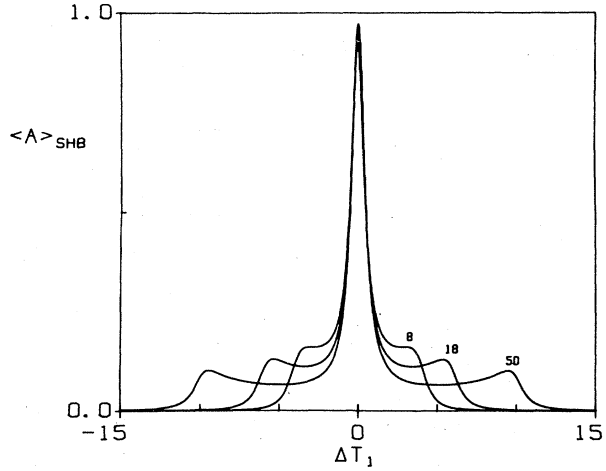

FIG. 9. Resonance-fluorescence spectra in a standing wave vs ΔT_1 for intensities I_2 of 8, 18, and 50 for each running wave. The ground state is the lower level and $T_2=2T_1$.

$$\langle A_{\rm EL}\rangle_{\rm SHB}=\frac{g^2(N_a-N_b)^2\pi I_2\mathcal{L}_2}{\gamma T_1(1+4I_2\mathcal{L}_2)^{3/2}}\delta(\Delta). \tag{44}$$

Because of the Lorentzians in the numerator and denominator of Eq. (44), the dependence of this expression on the detuning $\omega-\nu_2$ is almost the same as for the plane-wave case of Eq. (25). The dependence on the intensity shows that this average elastic peak also bleaches to zero for large fields, only now at a rate going like the inverse square root of the intensity, instead of the inverse of the intensity.

V. GAUSSIAN BEAMS

Actual lasers have transverse-field variations that can be closely approximated by a Gaussian beam.[17] This sometimes leads to the emergence of new phenomena not present for plane waves, such as self-focusing. In this section we assume the same Gaussian transverse profile for the strong-field intensity I_2 and the weak probe waves. We average the four coefficients A_1, B_1, C_1, and D_1 over this Gaussian dependence. Diffraction effects are not considered. The model includes an aperture of radius a. The limit $a\to 0$ reproduces the plane-wave result, since the medium is then everywhere saturated by the same value. The limit $a\to\infty$ gives the Gaussian-averaged result.

The total electric field is

$$E(r,z,t)=\left[\tfrac{1}{2}\mathcal{E}U(r)\sum_n a_n(t)e^{-i(\nu_n t-K_n z)}\right]+\text{H.c.}, \tag{45}$$

where $\mathcal{E}$ is the "electric field per photon," and we take the transverse spatial factor to be

$$U(r)=e^{-r^2/2w_0^2}. \tag{46}$$

Here $r=(x^2+y^2)^{1/2}$ is the radial coordinate and w_0 is the beam waist. This gives the radially dependent pump intensity

$$I_{2r}=I_2e^{-r^2/w_0^2}\equiv I_2u(r). \tag{47}$$

The average of the A_1 coefficient is then given by

$$\langle A_1\rangle_{\rm GB}=\frac{1}{N_1}\int_0^a dr\, re^{-r^2/w_0^2}A_1(r)\,, \tag{48}$$

where N_1 is the normalization factor

$$N_1=\int_0^a dr\, r\, e^{-r^2/w_0^2}=\frac{w_0^2}{2}(1-u_a)\,, \tag{49}$$

with $u_a\equiv u(a)=e^{-a^2/w_0^2}$. This is similar to the average over spatial hole burning of Sec. IV because we are again considering variations of the intensity. Unlike the spatial hole burning problem we now consider the variation to be in the transverse direction instead of the longitudinal direction. The dependence upon the intensity can again be separated and the same notation can be used. By using $u(r)$ as the variable of integration the resulting integrals can be readily integrated. The results are

$$\langle A_1\rangle_{\rm GB}=\frac{g^2\mathscr{D}_1}{I_2(1-u_a)}\left\{\frac{N_a\mathscr{L}_2^2-b_1\mathscr{L}_2+c}{\mathscr{L}_2-d}\left[\frac{1}{\mathscr{L}_2^2}\ln\left[\frac{1+I_2\mathscr{L}_2}{1+I_2\mathscr{L}_2u_a}\right]-\frac{1}{d^2}\ln\left[\frac{1+I_2d}{1+I_2du_a}\right]\right]+\frac{cI_2}{d\mathscr{L}_2}(1-u_a)\right\}, \tag{50}$$

$$\langle B_1\rangle_{\rm GB}=\frac{g^2\mathscr{D}_1}{I_2(1-u_a)}\left\{\frac{N_b\mathscr{L}_2^2-b_2\mathscr{L}_2+c}{\mathscr{L}_2-d}\left[\frac{1}{\mathscr{L}_2^2}\ln\left[\frac{1+I_2\mathscr{L}_2}{1+I_2\mathscr{L}_2u_a}\right]-\frac{1}{d^2}\ln\left[\frac{1+I_2d}{1+I_2du_a}\right]\right]+\frac{cI_2}{d\mathscr{L}_2}(1-u_a)\right\}, \tag{51}$$

$$\langle C_1\rangle_{\rm GB}=-\frac{g^2U_1^*U_3^*\mathscr{D}_1}{I_2(1-u_a)}\left\{\frac{-b_3\mathscr{L}_2+c}{\mathscr{L}_2-d}\left[\frac{1}{\mathscr{L}_2^2}\ln\left[\frac{1+I_2\mathscr{L}_2}{1+I_2\mathscr{L}_2u_a}\right]-\frac{1}{d^2}\ln\left[\frac{1+I_2d}{1+I_2du_a}\right]\right]+\frac{cI_2}{d\mathscr{L}_2}(1-u_a)\right\}, \tag{52}$$

$$\langle D_1\rangle_{\rm GB}=-\frac{g^2U_1^*U_3^*\mathscr{D}_1}{I_2(1-u_a)}\left\{\frac{-b_4\mathscr{L}_2+c}{\mathscr{L}_2-d}\left[\frac{1}{\mathscr{L}_2^2}\ln\left[\frac{1+I_2\mathscr{L}_2}{1+I_2\mathscr{L}_2u_a}\right]-\frac{1}{d^2}\ln\left[\frac{1+I_2d}{1+I_2du_a}\right]\right]+\frac{cI_2}{d\mathscr{L}_2}(1-u_a)\right\}, \tag{53}$$

where b_1, b_2, b_3, b_4, c, and d are given by Eqs. (36)–(41), respectively. We can again take the differences $\langle A_1-B_1\rangle_{\rm GB}$ and $\langle C_1-D_1\rangle_{\rm GB}$ to compare to previously derived semiclassical results.[9] The results are

$$\langle A_1-B_1\rangle_{\rm GB}=\frac{g^2\mathscr{D}_1(N_a-N_b)}{I_2(1-u_a)}\left[\left[\mathscr{L}_2-\mathscr{F}\frac{\gamma}{2}(\mathscr{D}_3^*-\mathscr{D}_2^*)\right]\frac{1}{\mathscr{L}_2}\ln\left[\frac{1+I_2\mathscr{L}_2}{1+I_2\mathscr{L}_2u_a}\right]-\frac{\mathscr{F}\gamma}{2}\frac{\mathscr{D}_1+\mathscr{D}_2^*}{d}\ln\left[\frac{1+I_2d}{1+I_2du_a}\right]\right], \tag{54}$$

$$\langle C_1-D_1\rangle_{\rm GB}=\frac{g^2U_1^*U_3^*\mathscr{D}_1(N_a-N_b)\mathscr{F}\frac{\gamma}{2}(\mathscr{D}_2+\mathscr{D}_3^*)}{I_2(1-u_a)}\left[\frac{1}{\mathscr{L}_2}\ln\left[\frac{1+I_2\mathscr{L}_2}{1+I_2\mathscr{L}_2u_a}\right]-\frac{1}{d}\ln\left[\frac{1+I_2d}{1+I_2du_a}\right]\right]. \tag{55}$$

These agree with the results of Ref. 9, Eqs. (30), and (31).

Figure 10 shows the resonance-fluorescence spectrum for the case of upper- to ground-level decay for the case of $T_1=T_2$ and an I_2 of 20 for the aperture values of 0.1, 1.0, and 20. For $a=0.1$, this corresponds to closing down the aperture in the center of the Gaussian beam until only of a small portion of the center is passed, which approximates a plane wave. We see this yields the familiar Mollow three-peaked spectrum.[11] As the aperture increases, more of the attenuated beam is passed, which has an effect similar to the spatial hole burning case of smoothing out the sidebands and increasing the central peak. The $a=20$ curve corresponds to a full Gaussian beam and it can be seen that the sidebands are washed out. For this case, $u_a\simeq 0$ in the above formulas. Note that unlike some kinds of Gaussian beam averages,[18] an effective plane-wave intensity cannot be used to approximate this case.

We evaluate the effects of a Gaussian beam on the elastic (Rayleigh) peak by inserting Eq. (25) into the integral of Eq. (48). The result is

$$\langle A_{\rm EL}\rangle_{\rm GB}=\frac{\pi g^2(N_a-N_b)^2}{2\gamma T_1I_2\mathscr{L}_2(1-u_a)}\left[\ln\left[\frac{1+I_2\mathscr{L}_2}{1+I_2\mathscr{L}_2u_a}\right]-\frac{I_2\mathscr{L}_2(1-u_a)}{(1+I_2\mathscr{L}_2)(1+I_2\mathscr{L}_2u_a)}\right]\delta(\Delta)\,. \tag{56}$$

In the limit $a\to 0$, this reduces to the plane wave Eq. (25). Figure 11 plots the Rayleigh peak versus the detuning $\omega-\nu_2$ for $I_2=20$, and $a=0.1$ and 20. In spite of the seeming complicated nature of Eq. (56) the curves of the figure show approximately the same behavior as for the plane-wave case. For each value of the aperture there is a sharp dip at zero detuning and then a gradual fall off for large detunings, just as for the plane-wave solution. As

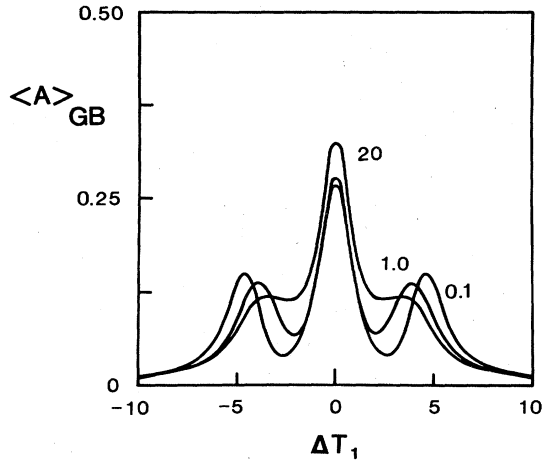

FIG. 10. Effects of different aperture sizes of Gaussian beams on the resonance fluorescence spectrum vs ΔT_1. The aperture sizes are $0.1w_0$, w_0, and $20w_0$. The pump intensity $I_2=20$, and $T_1=T_2$.

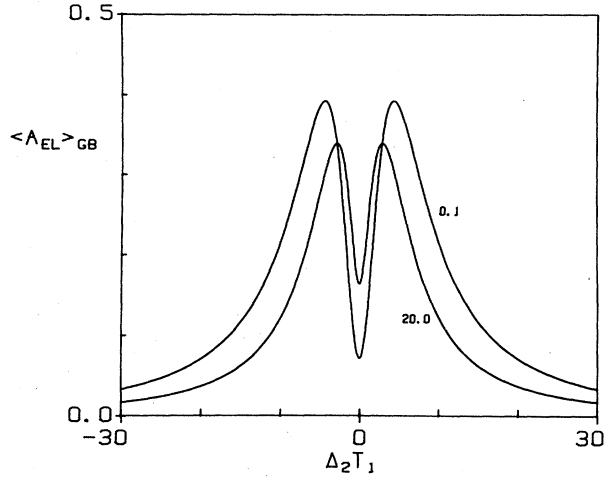

FIG. 11. The intensity of the elastic (Rayleigh) contribution vs the detuning $\Delta_2=\delta=(\omega-\nu_2)$ for the aperture sizes of $0.1w_0$ and $20\omega_0$. Same parameters as Fig. 10.

the aperture a increases the drop at line center decreases, but there is a lower maximum elastic intensity and a faster fall off for larger detunings. These results are expected since a Gaussian beam has a lower overall intensity than a plane wave.

VI. CONCLUSION

This paper extends the results of Refs. 1 and 2 to include inhomogeneous broadening, spatial hole burning, and Gaussian beams. We illustrate the results by considering the effects on resonance fluorescence. We find that the detuned resonance-fluorescence spectrum is markedly different for the two kinds of two-level media we have considered. We also find that Rayleigh scattering in the purely excited-state two-level model is negligible. Both of these results stem from the $\mathscr{S}/i\Delta$ term in the expression for A_1. In Ref. 1 this term is shown to be related to the off-diagonal matrix element of the field density operator ρ. In all cases we find that even for small amounts of inhomogeneous broadening there is a noticeable alteration of the shape of the spectrum.

The averages over spatial hole burning reveal a washout of the resonance-fluorescence side Lorentzians. In addition, they will be used in subsequent papers dealing with effects of noise in four-wave mixing and standing-wave cavity effects occurring in saturation spectroscopy.[13] These results are particularly important since they will be used to study new, quantum-mechanical phenomena. The Gaussian beam results may give clues to how real experimental data may be affected.

ACKNOWLEDGMENTS

It is a pleasure to thank Matthew Derstine and Darwin Sanders for their indispensable assistance in developing the *C*-language software able to graph all equations in this paper on an IBM Personal Computer. The work of two of us (D.A.H. and M.S.) was supported in part by the U.S. Office of Naval Research under Contract No. N00014-81-K-0754.

[1]M. Sargent III, D. A. Holm, and M. S. Zubairy, Phys. Rev. A **31**, 3112 (1985). The two excited-state case was presented by M. Sargent III, M. S. Zubairy, and F. DeMartini, Opt. Lett. **8**, 76 (1983).

[2]S. Stenholm, D. A. Holm, and M. Sargent III, Phys. Rev. A **31**, 3124 (1985).

[3]For a large anotated bibliography of papers on optical instabilites, see N. B. Abraham, L. A. Lugiato, and L. M. Narducci, J. Opt. Soc. Am. B **2**, 7 (1985).

[4]Instabilities involving inhomogeneous broadening were predicted and studied by L. W. Casperson and by N. B. Abraham and co-workers. For new work and references to the older work, see M. L. Minden and L. W. Casperson, J. Opt. Soc. Am. B **2**, 120 (1985); and also L. M. Hoffer, T. H. Chyba, and N. B. Abraham, *ibid.* **2**, 102 (1985).

[5]For theoretical work pertinent to the current calculations, see S. T. Hendow and M. Sargent III, J. Opt. Soc. Am. B **2**, 84 (1985); see also P. Mandel, *ibid.* **2**, 112 (1985).

[6]For a review of two-photon Doppler-free spectroscopy, see E. Giacobino and B. Cagnac, in *Progress in Optics,* edited by E. Wolf (North-Holland, Amsterdam, 1980), Chap. 2.

[7]R. L. Abrams and R. C. Lind, Opt. Lett. **2**, 94 (1978); **3**, 205 (1978).

[8]T. Fu and M. Sargent III, Opt. Lett. **4**, 366 (1979).

[9]For semiclassical calculations corresponding to the present work and further references on Gaussian beam effects, see S. Stuut and M. Sargent III, J. Opt. Soc. Am. B **1**, 95 (1984).

[10]For discussion relevant to laser instabilities, see L. A. Lugiato and M. Milani, J. Opt. Soc. Am. B **2**, 120 (1985).

[11]B. R. Mollow, Phys. Rev. **188**, 1969 (1969).

[12]J. D. Cresser, J. Häger, G. Leuchs, M. Rateike, and H. Walther, in *Dissipative Systems in Quantum Optics,* edited by R. Bonafacio (Springer, Berlin, 1982), Chap. 3.

[13]D. A. Holm, M. Sargent III, and S. Stenholm, J. Opt. Soc. Am. B (to be published).

[14]M. Sargent III, M. O. Scully, and W. E. Lamb, Jr., *Laser*

Physics (Addison-Wesley, Reading, MA, 1974).

[15]For a general review of the semiclassical theory of saturation spectroscopy corresponding to the quantum treatment of the present paper, see M. Sargent III, Phys. Rep. **43C**, 223 (1978).

[16]D. A. Holm and M. Sargent III, in *Coherence and Quantum Optics V,* edited by L. Mandel and E. Wolf (Plenum, New York, 1984).

[17]See, for example, A. Yariv, *Introduction to Optical Electronics* (Holt, Rinehart and Winston, New York, 1976).

[18]M. Sargent III, J. Appl. Phys. **48**, 243 (1977).